

Identification of hNopp140 as a Binding Partner for Doxorubicin with a Phage Display Cloning Method

Youngnam Jin,¹ Jaehoon Yu,² and Yeon Gyu Yu^{1,3}

¹Structural Biology Center

²Medicinal Chemistry Research Center

Korea Institute of Science and Technology

P.O. Box 131

Cheongryang, Seoul 130-650

Korea

Summary

Doxorubicin is a widely used anti-cancer drug. It is assumed to act by inhibiting DNA replication or transcription, although its precise targets and mechanism of cytotoxicity remain unresolved. A T7 phage library expressing human liver cDNA was screened against immobilized doxorubicin to isolate doxorubicin binding proteins. The selected phage contained the C-terminal region of nucleolar phosphoprotein hNopp140, an important factor in the biogenesis of the nucleolus. When the cloned sequence was expressed in *E. coli*, the recombinant protein was phosphorylated by casein kinase II and oligomerized in the presence of magnesium and fluoride ions, as occurs in vivo. Doxorubicin bound to the expressed protein with a dissociation constant of 4.5×10^{-6} M, and this interaction was inhibited by the phosphorylation of hNopp140. These results suggested that doxorubicin might disrupt the cellular function of hNopp140.

Introduction

Doxorubicin is one of the anthracycline antibiotics isolated from *Streptomyces*. It is composed of an anthracycline ring linked via a glycosidic bond to an amino sugar. It is an antineoplastic agent used for the treatment of acute leukemia and a wide variety of solid tumors [1], although it has been associated with severe side effects such as nausea, local necrosis, anorexia, and alopecia [2, 3]. The four fused-ring structure of doxorubicin pointed to its major target as being chromosomal DNA, where it intercalates between the base pairs. Doxorubicin can bind to supercoiled plasmid DNA or calf thymus DNA with dissociation constants in the 10^{-5} M range [4]. The intercalation would hinder DNA replication or transcription [5, 6] and also affect the activity of DNA-modifying enzymes, including topoisomerase [7].

Although the DNA binding appears to be critical for the anticancer activity of doxorubicin, the detailed cytotoxic mechanism of its action is not yet fully understood. There have been reports of doxorubicin interacting with cellular components other than DNA. The activity of RNA polymerase II with either denatured or native DNA as a template was inhibited with similar sensitivities by doxorubicin [8]. It has been reported also that the generation of active oxygen species from doxorubicin contrib-

utes to its cytotoxicity [9–11] and that the interaction of doxorubicin with an extracellular component(s) induces a toxic effect [12–14]. Together, these observations imply that doxorubicin could interact with a variety of cellular components, some of which may be the targets for its anticancer activity.

Methods to identify proteins that interact with a specific ligand are limited. An affinity selection method in which the target proteins are purified from cell extracts by the use of ligand-immobilized beads has been described. FKBP12 (FK506 binding protein) is an example that was isolated from a whole-cell extract by the use of immobilized FK506 on resin beads [15]. Biopanning by using a phage display library provides another method for the identification of the target proteins to specific ligands. Random sequences of hepta- or dodecameric peptides [16, 17] or cDNA from human tissue [18, 19] can be displayed on the surface of phage particles. Such phage libraries have been used successfully to identify proteins that specifically bind to immobilized taxol [20] or FK506 [21].

This study has identified a doxorubicin-interacting protein by using a phage library displaying human liver cDNA. A phage clone expressing the C-terminal domain of human nucleolar phosphoprotein, hNopp140, was selectively amplified during the biopanning procedure. Furthermore, the expressed protein showed specific binding to doxorubicin in a phosphorylation-dependent manner.

Results

Doxorubicin-Specific Phage Was Amplified by Biopanning

A T7 phage library displaying human liver cDNA was screened for proteins binding specifically to the biotinylated doxorubicin (Figure 1) on a streptavidin-coated plate. The phage titer of the eluted solutions increased from 10^3 pfu/ml after the first round to 10^5 pfu/ml at the fourth round of binding and elution (Figure 2A). To confirm the enrichment of specific phage particles, cDNAs inserted into the eluted phages were analyzed by PCR with primers flanking the library construction site of the T7 phage DNA. The phage PCR products from the first round of elution appeared as smear bands (Figure 2B, lane 1). The PCR products of the eluted phages from the second-, third-, and fourth-round amplifications (Figure 2B, lanes 2, 3, and 4), however, revealed bands of 600 and 870 bp. These results indicated that doxorubicin-specific phages were selectively amplified by the biopanning procedure.

Sequence Analysis of Doxorubicin-Specific Phage Clone

DNA sequences were determined for 20 phages eluted and selected from the fourth and final round of biopanning. Two of the isolated clones had a PCR product of 870 bp and had an insert of 648 bp that produced an open reading frame of 216 amino acids. The other 18

³ Correspondence: ygy@kist.re.kr

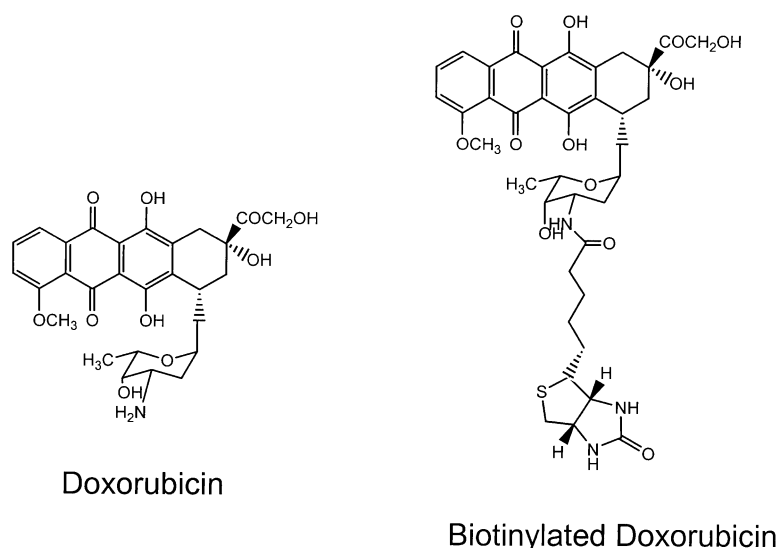


Figure 1. Structure of Doxorubicin and Biotinylated Doxorubicin

The amine group of doxorubicin was coupled with NHS-biotin to produce biotinylated doxorubicin.

clones had PCR products of about 600–700 bp. However, the ORFs from these clones consisted of less than 20 amino acids. These clones represented background binders, and they were not further analyzed. The sequence of the ORF of 216 amino acids was identical to the C-terminal region (amino acids 388–603 out of 699 residues) of human nucleolar phosphoprotein, hNopp140. When the phage plaques from each round of elution were hybridized with the cloned DNA as a probe, the phage containing the hNopp140 sequence was enriched during the biopanning procedure (data not shown).

Expression and Characterization of the C-Terminal Region of hNopp140

The cloned sequence of hNopp140 was expressed and purified to examine its interaction with doxorubicin. It was inserted at the C terminus of thioredoxin, and the fusion protein (Trx-hNopp140C) was overexpressed in *E. coli* in a soluble form. The protein was further purified by Ni affinity and hydroxylapatite columns (Figure 3A, lane 1). The protein hNopp140 has more than 80 potential phosphorylation sites and is highly phosphorylated by casein kinase II [22]. When the purified Trx-hNopp140C was treated with calf intestine phosphatase, it comigrated with the untreated protein in SDS-

PAGE (Figure 3A, lanes 1 and 2) and urea gels (Figure 3C, lanes 1 and 2). In contrast, the protein treated with casein kinase II migrated more slowly than the native form in SDS-gels (Figure 3A, lane 3) and was radio-labeled by ^{32}P ATP in a phosphorylation reaction (Figure 3B). The phosphorylated form migrated more quickly than the native form in urea-denaturing gels because of the increased negative charge (Figure 3C, lane 3). These results indicate that the recombinant hNopp140 protein was comparable in conformation to the native form since both can be similarly phosphorylated by casein kinase II.

It has been shown that hNopp140 aggregates to an insoluble form in the presence F^- and Mg^{2+} ions [23]. To examine the involvement of the cloned C-terminal region of hNopp140 in the aggregation, we tested the solubility of Trx-hNopp140C in the presence of NaF and MgCl_2 salts. The unphosphorylated form of Trx-hNopp140C was not aggregated (Figure 4, lane 1 and 2). In contrast, most of the phosphorylated protein was aggregated and insoluble (Figure 4, lanes 3 and 4). These results indicate that the cloned region of hNopp140 is responsible for the salt-dependent oligomerization and that this phenomenon is negatively controlled by phosphorylation.

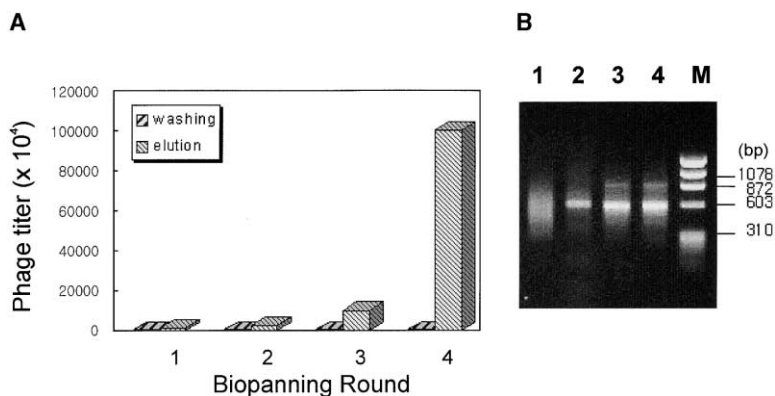


Figure 2. Analysis of Phages Eluted after Each Round of Biopanning

(A) The phage titer was determined for each washing and eluted solution at each round. (B) The insert size of the phage DNA from the whole eluted phage sample at each round was analyzed by polymerase chain reaction (PCR) with primers flanking the insertion sites. The PCR products from the first-, second-, third-, and fourth-round elutions were loaded in lanes 1, 2, 3, and 4, respectively, along with marker DNA (lane M).

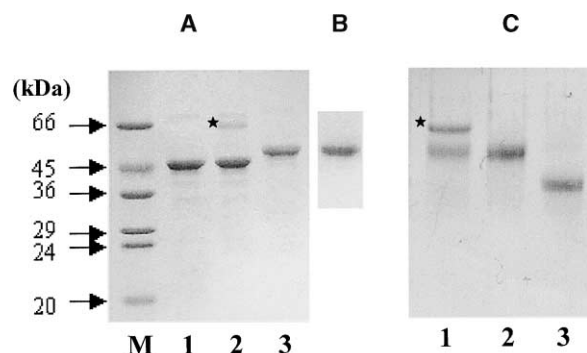


Figure 3. Phosphorylation of the Purified Trx-hNopp140C

(A) The native form of Trx-hNopp140C (lane 1), along with the dephosphorylated (lane 2) and phosphorylated (lane 3) forms, was analyzed by 12% SDS-gel electrophoresis.

(B) When ^{32}P -d-ATP was used in the phosphorylation reaction, Trx-hNopp140C was labeled with ^{32}P .

(C) Dephosphorylated (lane 1), native (lane 2), and phosphorylated forms (lane 3) of Trx-hNopp140C were analyzed by 8% Urea-PAGE. The marked band in lane 2 of panel (A) and in lane 1 of panel (C) was calf intestine phosphatase (dephosphorylating enzyme).

Direct Measurement of the Binding between Doxorubicin and Trx-hNopp140C

The interaction between doxorubicin and Trx-hNopp140C was analyzed by fluorescence spectrometry and surface plasmon resonance analysis. Doxorubicin had an emission spectrum of 530–600 nm with a peak at 555 nm. The addition of the recombinant Trx-hNopp140C protein in a dose-dependent manner significantly increased the emission intensity, although the shape of spectrum was almost unchanged (Figure 5). BSA or thioredoxin, however, had no effect on the fluorescence spectrum (data not shown). Interestingly, phosphorylated Trx-hNopp140C also had no effect on the fluorescence spectrum of doxorubicin, suggesting that doxorubicin could interact only with dephosphory-

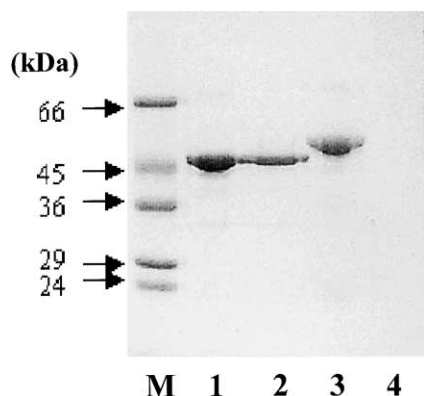


Figure 4. Phosphorylation-Dependent Aggregation of Trx-hNopp140C

The formation of insoluble aggregates of Trx-hNopp140C was examined after incubation with 25 mM each of NaF and MgCl_2 at 4°C for 1 hr. Native (lane 1 and 2) or phosphorylated Trx-hNopp140C (lanes 3 and 4) was incubated in the presence (lanes 2 and 4) or absence (lanes 1 and 3) of NaF and MgCl_2 , and the soluble fraction was analyzed by 12% SDS-PAGE.

lated hNopp140C. When Trx-hNopp140C was applied to immobilized doxorubicin on the CM5 surface plasmon resonance sensor chip, a strong binding curve was observed (Figure 6). The apparent dissociation constant (K_d) of Trx-hNopp140C binding to doxorubicin was calculated as 4.5×10^{-6} M. As in the fluorescence measurement experiment, the phosphorylated form of Trx-hNopp140C failed to bind doxorubicin. When the 650 bp DNA fragment (100 nM) was applied to the chip surface, no significant adsorption curve was observed. These results imply that doxorubicin binds specifically to the nonphosphorylated form of hNopp140, with a higher binding affinity than for DNA.

Discussion

Different phage libraries have been developed to display short peptides of 7–12 amino acids [16, 17, 24] as well as larger proteins up to 40 kDa [25] as fusion proteins of the P3 or P8 M13 phage coat protein. In addition, the p10 coat protein of the T7 phage was used to display proteins up to 1000 amino acids. Biopanning with these phage display libraries has been used to identify peptide motifs that bind specifically to a particular receptor [26, 27], enzyme [28, 29], or even RNA [30]. In addition, the p10 coat protein of the T7 phage was used to display proteins up to 1000 amino acids, and such a display library has been successfully used for the identification of proteins that interact with specific protein or synthetic peptides [31]. This method was also applied to identify small-molecule interactors, such as FK506 or taxol [20, 21]. In this study, a C-terminal region of hNopp140 was selected and identified as an interacting protein of doxorubicin by the biopanning procedure from the T7 phage display library displaying human liver cDNA. The expressed C-terminal region of hNopp140 showed strong binding affinity for doxorubicin, with an apparent dissociation constant in the μM range.

The ring moiety in doxorubicin comprises the probable binding motif for hNopp140 since the sugar group was used for immobilization. This was supported by the increased fluorescence intensity of doxorubicin in the presence of hNopp140. Since the fluorescent chromophore is the ring moiety, the change of fluorescence indicated that hNopp140 directly contacted the ring group and might contribute to the dequenching effect. The affinity of doxorubicin for hNopp140 appeared to be stronger than its affinity for DNA. The reported dissociation constant for doxorubicin/DNA binding (about 10–20 μM ; [4]) is 2- to 5-fold higher than the observed value for the binding of immobilized doxorubicin and Trx-hNopp140C in this study. Furthermore, a double-stranded DNA fragment failed to show any significant binding to the immobilized doxorubicin in our BIAcore study (Figure 5). The 3' amino group of doxorubicin participates in the interaction with DNA [32] and forms a covalent link with the 2-amino group in guanine [33]. Hence, the failure of the DNA to associate with the immobilized doxorubicin in these experiments might be due to the lack of the free 3' amino group on doxorubicin.

The specific binding between doxorubicin and hNopp140 suggests that the drug might interact prefer-

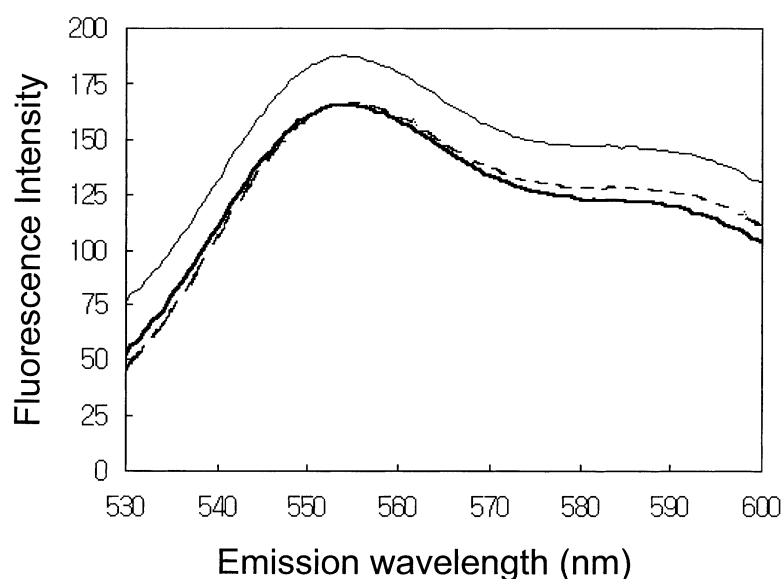


Figure 5. Fluorescence Spectra of Doxorubicin and Trx-P140C/Doxorubicin Complex

The fluorescence spectrum of 0.7 μ M doxorubicin alone (bold line) in 10 mM Mops buffer containing 150 mM NaCl and 0.5 mM EDTA (pH 7.5) was compared with the spectrum of doxorubicin in the presence of 10 μ M native (thin line) or phosphorylated forms of Trx-hNopp140C (dotted line). The excitation wavelength was 490 nm, and the emission spectrum was obtained between 530 and 600 nm.

entially with hNopp140 after in vivo administration and thereby affect the cellular function of hNopp140. Previously, mouse Nopp140 was known to be located at the nucleolus, and it was assumed to be a key component in the biogenesis of nucleoli [22]. It was also shown to interact with proteins involved in the transcription of rDNA; such proteins included RNA polymerase I [34], C/EBP [35], and casein kinase II [36]. hNopp140 was identified as one of the most highly phosphorylated proteins and possessed ATPase/GTPase activity [23]. Overexpression of the partial or whole hNopp140 cDNA resulted in mislocalization of nucleolar proteins, improper formation of the nucleolus, and inhibition of rRNA gene transcription [34, 37].

It should be noted that the cell cycle stage at which doxorubicin has an effect is synchronous to a stage when the expression of hNopp140 is reduced. Doxorubicin has been known to arrest the cell cycle at the G2/M phase. hNopp140 levels are decreased during mitosis, and the remaining hNopp140 in mitotic cells can be

further phosphorylated [22]. Specific binding of doxorubicin to nonphosphorylated hNopp140 would affect the cellular function of hNopp140, such as in ribosomal assembly or transcription of rDNA, and severely affect the normal operation of the cell cycle.

Conclusions and Future Work

We have cloned the C-terminal domain of hNopp140 as a doxorubicin binding protein by using a phage display cloning method. Fluorescence spectrometry confirmed that the expressed protein binds to doxorubicin, and we used surface plasmon resonance to measure a dissociation constant. Furthermore, it was shown that the only the unphosphorylated form of hNopp140 was bound. From these results, it can be implied that doxorubicin affects the cellular function of hNopp140. Since hNopp140 plays a critical role in the rDNA transcription and the biogenesis of nucleolus, the binding of doxorubicin to hNopp140 would severely affect cell growth. A detailed analysis of the localization, cellular levels, and

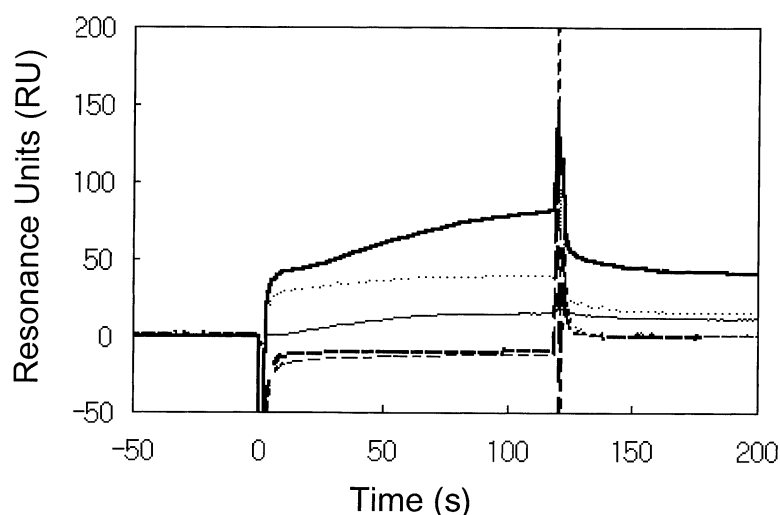


Figure 6. The Binding Sensorgram of the C-Terminal Region of hNopp140 on Doxorubicin

Sensorgrams were obtained for 62.5 nM (thin line), 1 μ M (dotted line), and 2 μ M (bold line) of Trx-hNopp140C, 4 μ M of phosphorylated Trx-hNopp140C (broken line), and 100 nM of DNA (bold broken line) against doxorubicin immobilized on the sensor chip.

possible conformational alterations to hNopp140 in doxorubicin-treated cells would elucidate the relationship between hNopp140 and the anti-cancer drug doxorubicin and contribute to a better understanding of the mechanism of this drug's cytotoxicity.

Significance

Display cloning has been developed for use with affinity selection methods to identify the cellular targets of bioactive compounds. The specific interaction demonstrated between the protein isolated from the human cDNA phage library and doxorubicin illustrates that this approach is effective for the identification of therapeutic targets as well as bioactive natural compounds.

Experimental Procedures

Materials

Doxorubicin hydrochloride was obtained from Aldrich (USA), the 96-well plate was coated with streptavidin, and NHS-biotin was purchased from Pierce (USA). The T7 phage library displaying a human liver cDNA library was purchased from Novagen (USA). Sensor chip CM5 and the Amine Coupling Kit were obtained from Applied Biochem. (Sweden). All other reagents were of reagent grade.

Immobilization of Doxorubicin and Biopanning

Doxorubicin was biotinylated after the incubation of 2 mM sulfo-NHS-biotin and 8 mM of doxorubicin in 50 mM sodium bicarbonate buffer (pH 8.0) at room temperature for 3 hr. Unreacted sulfo-NHS-biotin was inactivated by incubation in the presence of 50 mM glycine (pH 8.0) for 1 hr. The mixture was then diluted 20-fold in PBS buffer (20 mM sodium phosphate buffer [pH 7.5] 150 mM NaCl) and transferred to a well of the streptavidin-coated plate. After incubation for 1 hr at room temperature, the well was washed six times with 0.1% Tween-20 solution in PBS buffer (PBST). The T7 phage library of human liver cDNA (6×10^9 pfu) in 100 μ l of PBS buffer was added to the doxorubicin-attached plate, and the plate was incubated at room temperature for 40 min with gentle shaking. The plate was washed ten times with PBST, and phage particles that adsorbed to the surface of the well were eluted after 30 min of incubation in the presence of 1% SDS. The eluted phage particles were amplified after infection into *E. coli* strain BLT5615 according to the manufacturer's instructions (Novagen). The amplified phage was applied to the streptavidin-coated plate primed with biotinylated doxorubicin. The phages that were bound to the surface were eluted by the use of 1% SDS in the scibd round and 2.5 mM biotin in the third and fourth rounds of biopanning. The biotin in the eluted phage solution was not specifically removed because its concentration was diluted to 5000-fold during the phage amplification procedure. The concentrations of NaCl and Tween-20 in the washing solution used in the second, third, and fourth rounds of elutions were increased to 170 mM, 200 mM, and 250 mM and 0.3%, 0.5%, and 0.7%, respectively. DNA was extracted from the isolated T7 phages with the Lambda Mini Kit (QIAGEN) and sequenced with the PRISM Dye Terminator Cycle Sequencing Ready Reaction Kit (Applied Biosystems). The BLAST program [38] was used for comparing the obtained sequences with sequences in GenBank.

Expression and Purification of the C-Terminal Domain of hNopp140

The C-terminal domain of hNopp140 (amino acids 388–603) of the isolated phages from the T7 human liver cDNA displayed library was amplified by PCR (polymerase chain reaction). The DNA fragment was inserted into the BamHI and HindIII site of the expression vector, pETrx, a pET28a (Novagen) derivative constructed by insertion of the thioredoxin gene into the NdeI and BamHI sites of pET28a. The resulting plasmid, pTxP140C, was transformed into *E. coli* strain BL21(DE3), and the thioredoxin fusion protein containing the

hNopp140 sequence at the C terminus was expressed after induction by 1 mM IPTG. The harvested *E. coli* cells were lysed with a French Pressor, and cell debris was removed by centrifugation at $15,000 \times g$ for 20 min. The crude extract was loaded onto an Ni-NTA column, and the bound proteins were eluted with 200 mM of imidazole solution (pH 7.0). The eluted proteins were dialyzed against 10 mM Mops [3-(N-morpholino) propanesulfonic acid] buffer (pH 7.5) and loaded onto a hydroxylapatite column. Proteins were eluted with a gradient of 300 ml of 20–300 mM sodium phosphate (pH 7.5). The eluted proteins were pooled, concentrated, and dialyzed against 10 mM MOPS buffer.

Protein Phosphorylation

Proteins were phosphorylated by mixing 5 μ g of substrate protein with 50 U of casein kinase II (New England BioLabs) in 20 μ l of kinase reaction buffer (20 mM Tris-HCl [pH 7.5], 50 mM KCl, 10 mM $MgCl_2$, and 2.5 mM ATP) at 30°C for 2 hr. Dephosphorylation was performed by incubation of 5 μ g of substrate protein with 5 U of calf intestine alkaline phosphatase (New England BioLabs) in 20 μ l of the reaction solution containing 5 mM Tris-HCl (pH 7.9), 10 mM $MgCl_2$, 10 mM NaCl, and 0.1 mM dithiothreitol at 37°C for 1 hr. The addition of 20 μ l of 2 \times SDS buffer terminated phosphorylation or dephosphorylation, and the reaction mixtures were analyzed by SDS-PAGE.

Fluorescence and Biosensor Analysis

Interaction between doxorubicin and protein was analyzed by fluorescence spectroscopy and biosensor analysis. The various concentrations of proteins were mixed with 0.7 μ M doxorubicin in 10 mM Mops (pH 7.5) containing 150 mM NaCl and 0.5 mM EDTA, and the fluorescence spectra were measured with a LS50B Luminescence Spectrometer (Perkin Elmer). The excitation wavelength was 490 nm, and the emission spectra were obtained over the range of 530–600 nm.

For biosensor analysis, doxorubicin was covalently linked to a CM5 sensor chip with the Amine Coupling Kit. The surface matrix was activated by a 10 min injection of an aqueous solution of 0.2 M N-ethyl-N'-(3-diethylaminopropyl)-carbodiimide (EDC) and 50 mM N-hydroxysuccinimide (NHS). Then, 500 μ M doxorubicin in 30 μ l of 10 mM sodium phosphate (pH 7.0) and 150 mM NaCl was injected into the sensor cells. All coupling reactions were done at a flow rate of 5 μ l/min. Remaining N-hydroxysuccinimide-ester groups were inactivated by injection of 1.0 M ethanolamine-HCl (pH 8.5) for 10 min. Protein samples in the running buffer (10 mM Mops (pH 7.5), 150 mM NaCl, and 1 mM EDTA) were injected at a flow rate of 30 μ l/min. Association and dissociation curves were obtained on a BIAcore 3000 (ABI, USA). The surface of the sensor chip was regenerated by injection of 10 μ l of the regeneration buffer (0.017% SDS, 30 mM NaCl, and 1.7 mM NaOH). The SPR response curves were analyzed with BIAcore EVALUATIONS software, version 3.1.

Received: June 14, 2001

Revised: October 1, 2001

Accepted: October 2, 2001

Acknowledgments

We thank Dr. Key-Sun Kim for his helpful discussion. This work was supported by grants from the Functional Analysis of the Human Genome in The 21C Frontier Research Program in Korea.

References

1. Blum, R.H., and Carter, S.K. (1974). Adriamycin. A new anticancer drug with significant clinical activity. *Ann. Intern. Med.* **80**, 249–259.
2. Rudolph, R., Stein, R.S., and Pattillo, R.A. (1976). Skin ulcers due to adriamycin. *Cancer* **38**, 1087–1094.
3. O'Bryan, R.M., Baker, L.H., Gottlieb, J.E., Rivkin, S.E., Balcerzak, S.P., Grummet, G.N., Salmon, S.E., Moon, T.E., and Hoogstraaten, B. (1977). Dose response evaluation of adriamycin in human neoplasia. *Cancer* **39**, 1940–1948.
4. Simpkins, H., Pearlman, L.F., and Thompson, L.M. (1984). Ef-

- fects of adriamycin on supercoiled DNA and calf thymus nucleosomes studied with fluorescent probes. *Cancer Res.* 44, 613–618.
5. Crooke, S.T., Duvernay, V.H., Galvan, L., and Prestayko, A.W. (1978). Structure-activity relationships of anthracyclines relative to effects on macromolecular syntheses. *Mol. Pharmacol.* 14, 290–298.
6. Meriwether, W.D., and Bachur, N.R. (1972). Inhibition of DNA and RNA metabolism by daunorubicin and adriamycin in L1210 mouse leukemia. *Cancer Res.* 32, 1137–1142.
7. Tewey, K.M., Rowe, T.C., Yang, L., Halligan, B.D., and Liu, L.F. (1984). Adriamycin-induced DNA damage mediated by mammalian DNA topoisomerase II. *Science* 226, 466–468.
8. Chuang, R.Y., and Chuang, L.F. (1979). Inhibition of chicken myeloblastosis RNA polymerase II activity by adriamycin. *Biochemistry* 18, 2069–2073.
9. Sinha, B.K., and Chignell, C.F. (1979). Binding mode of chemically activated semiquinone free radicals from quinone anticancer agents to DNA. *Chem. Biol. Interact.* 28, 301–308.
10. Berlin, V., and Haseltine, W.A. (1981). Reduction of adriamycin to a semiquinone-free radical by NADPH cytochrome P-450 reductase produces DNA cleavage in a reaction mediated by molecular oxygen. *J. Biol. Chem.* 256, 4747–4756.
11. Keizer, H.G., Pinedo, H.M., Schuurhuis, G.J., and Joenje, H. (1990). Doxorubicin (adriamycin): a critical review of free radical-dependent mechanisms of cytotoxicity. *Pharmacol. Ther.* 47, 219–231.
12. Tritton, T.R., and Yee, G. (1982). The anticancer agent adriamycin can be actively cytotoxic without entering cells. *Science* 217, 248–250.
13. Hasmann, M., Valet, G.K., Tapiero, H., Trevorrow, K., and Lampidis, T. (1989). Membrane potential differences between adriamycin-sensitive and -resistant cells as measured by flow cytometry. *Biochem. Pharmacol.* 38, 305–312.
14. Jeannesson, P., Trentesaux, C., Gerard, B., Jardillier, J.-C., Ross, K.L., and Tokes, Z.A. (1990). Induction of erythroid differentiation in human leukemia K-562 cells by membrane-directed action of adriamycin covalently bound to microspheres. *Cancer Res.* 50, 1231–1236.
15. Harding, M.W., Galat, A., Uehling, D.E., and Schreiber, S.L. (1989). A receptor for the immunosuppressant FK506 is a cis-trans peptidyl-prolyl isomerase. *Nature* 341, 758–760.
16. Scott, J.K., and Smith, G.P. (1990). Searching for peptide ligands with an epitope library. *Science* 249, 386–390.
17. Clackson, T., and Wells, J.A. (1994). In vitro selection from protein and peptide libraries. *Trends Biotechnol.* 12, 173–184.
18. Cramer, R., Jaussi, R., Menz, G., and Blaser, K. (1994). Display of expression products of cDNA libraries on phage surfaces: a versatile screening system for selective isolation of genes by specific gene-product/ligand interaction. *Eur. J. Biochem.* 226, 53–58.
19. Jespers, L.S., De Keyser, A., and Stanssens, P.E. (1996). LambdaZLG6: a phage lambda vector for high efficiency cloning and surface expression of cDNA libraries on filamentous phage. *Gene* 173, 179–181.
20. Rodi, D.J., Janes, R.W., Sanganee, H.J., Holton, R.A., Wallace, B.A., and Makowski, L. (1999). Screening of a library of phage-displayed peptides identifies human Bcl-2 as a taxol-binding protein. *J. Mol. Biol.* 285, 197–203.
21. Sche, P.P., McKenzie, K.M., White, J.D., and Austin, D.J. (1999). Display cloning: functional identification of natural product receptors using cDNA-phage display. *Chem. Biol.* 6, 707–716.
22. Pai, C.Y., Chen, H.K., Sheu, H.L., and Yeh, N.H. (1995). Cell cycle-dependent alterations of a highly phosphorylated nucleolar protein p130 are associated with nucleologenesis. *J. Cell Sci.* 108, 1911–1920.
23. Chen, H.K., and Yeh, N.H. (1997). The nucleolar phosphoprotein P130 is a GTPase/ATPase with intrinsic property to form large complexes triggered by F^- and Mg^{2+} . *Biochem. Biophys. Res. Commun.* 230, 370–375.
24. Greenwood, J., Willis, A.E., and Perham, R.N. (1991). Multiple display of foreign peptides on a filamentous bacteriophage. Peptides from *Plasmodium falciparum* circumsporozoite protein as antigens. *J. Mol. Biol.* 220, 821–827.
25. Sidhu, S.S., Weiss, G.A., and Wells, J.A. (2000). High copy display of large proteins on phage for functional selections. *J. Mol. Biol.* 296, 487–495.
26. Szardenings, M., Muceniece, R., Mutule, I., Mutulis, F., and Wikberg, J.E. (2000). New highly specific agonistic peptides for human melanocortin MC(1) receptor. *Peptides* 21, 239–243.
27. Chang, C.Y., Norris, J.D., Grøn, H., Paige, L.A., Hamilton, P.T., Kenan, D.J., Fowlkes, D., and McDonnell, D.P. (1999). Dissection of the LXXLL nuclear receptor-coactivator interaction motif using combinatorial peptide libraries: discovery of peptide antagonists of estrogen receptors alpha and beta. *Mol. Cell. Biol.* 19, 8226–8239.
28. Hyde-DeRuyscher, R., Paige, L.A., Christensen, D.J., Hyde-DeRuyscher, N., Lim, A., Fredericks, Z.L., Kranz, J., Gallant, P., Zhang, J., Rocklage, S.M., et al. (2000). Detection of small-molecule enzyme inhibitors with peptides isolated from phage-displayed combinatorial peptide libraries. *Chem. Biol.* 7, 17–25.
29. O'Boyle, D.R., Pokornowski, K.A., McCann, P.J., and Weinheimer, S.P. (2000). Identification of a novel peptide substrate of HSV-1 protease using substrate phage display. *Virology* 236, 338–347.
30. Agris, P.F., Marchbank, M.T., Newman, W., Guenther, R., Ingram, P., Swallow, J., Mucha, P., Szyk, A., Rekowski, P., Peletskaya, E., et al. (1999). Experimental models of protein-RNA interaction: isolation and analyses of tRNA(Phe) and U1 snRNA-binding peptides from bacteriophage display libraries. *J. Protein Chem.* 18, 425–435.
31. Zozulya, S., Lioubin, M., Hill, R.J., Abram, C., and Gishizky, M.L. (1999). Mapping signal transduction pathways by phage display. *Nature Biotech.* 17, 1193–1198.
32. Kellogg, G.E., Scarsdale, J.N., and Fornari, F.A., Jr. (1998). Identification and hydropathic characterization of structural features affecting sequence specificity for doxorubicin intercalation into DNA double-stranded polynucleotides. *Nucleic Acids Res.* 26, 4721–4732.
33. Zeman, S.M., Phillips, D.R., and Crothers, D.M. (1998). Characterization of covalent adriamycin-DNA adducts. *Proc. Natl. Acad. Sci. USA* 95, 11561–11565.
34. Chen, H.K., Pai, C.Y., Huang, J.Y., and Yeh, N.H. (1999). Human Nopp140, which interacts with RNA polymerase I: implications for rRNA gene transcription and nucleolar structural organization. *Mol. Cell. Biol.* 19, 8536–8546.
35. Miao, L.H., Chang, C.J., Tsai, W.H., and Lee, S.C. (1997). Identification and characterization of a nucleolar phosphoprotein, Nopp140, as a transcription factor. *Mol. Cell. Biol.* 17, 230–239.
36. Li, D., Meier, U.T., Dobrowolska, G., and Krebs, E.G. (1997). Specific interaction between casein kinase 2 and the nucleolar protein Nopp140. *J. Biol. Chem.* 272, 3773–3779.
37. Isaac, C., Yang, Y., and Meier, U.T. (1998). Nopp140 functions as a molecular link between the nucleolus and the coiled bodies. *J. Cell Biol.* 142, 319–329.
38. Altschul, S.F., Madden, T.L., Schaffer, A.A., Zhang, J., Zhang, Z., Miller, W., and Lipman, D.J. (1997). Gapped BLAST and PSI-BLAST: a new generation of protein database search programs. *Nucleic Acids Res.* 25, 3389–3402.